Journal of Applied Physics ARTICLE scitation.org/journal/jap

Piezoelectric P(VDF-TrFE) film inkjet printed on silicon for high-frequency ultrasound applications

Cite as: J. Appl. Phys. **129**, 195107 (2021); doi: 10.1063/5.0048444
Submitted: 23 February 2021 · Accepted: 6 May 2021 ·
Published Online: 20 May 2021

View Online Export Citation CrossMark

Aline Banquart,[1,2,3,a)] Samuel Callé,[2] Franck Levassort,[2] Lionel Fritsch,[4,b)] Frédéric Ossant,[1] Sean Toffessi Siewe,[1,2,3] Stéphanie Chevalliot,[3] Arnaud Capri,[3] and Jean-Marc Grégoire[1]

AFFILIATIONS

[1]UMR 1253, iBrain, Université de Tours, Inserm, 37000 Tours, France
[2]GREMAN UMR 7347, Université de Tours, CNRS, INSA CVL, 37100 Tours, France
[3]Carestream Dental France, 77183 Croissy-Beaubourg, France
[4]Irlynx SA, 38240 Meylan, France

[a)]**Author to whom correspondence should be addressed:** aline.banquart@univ-tours.fr
[b)]**Present address:** LFritsch-Technologies Consulting, 38383 St Etienne de Crossey, France.

ABSTRACT

We investigated the innovative processing of poly(vinylidene fluoride-trifluoroethylene) P(VDF_x-$TrFE_{1-x}$) ($x = 83$ mol. %) by inkjet printing to deliver uniform and thickness-controlled layers on silicon substrates. Here, we provide detailed processing steps and optimize film deposition conditions. The thickness coupling factor for a P(VDF-TrFE) film around 11 μm thick was 22%, demonstrating good electromechanical performance after poling. These multilayer structures were specifically for high-frequency, single-element ultrasonic transducer applications. The measurements of electro-acoustic responses were in water. The maximal frequency was centered at 33.2 MHz and had a fine axial resolution at 22 μm, corresponding to a fractional bandwidth at −6 dB of 100%. In the context of technological evolutions aimed at miniaturized devices and integrated electronics, these results allow for the consideration of complex structures such as multi-element transducers for high-frequency imaging applications.

Published under an exclusive license by AIP Publishing. https://doi.org/10.1063/5.0048444

I. INTRODUCTION

Poly(vinylidene fluoride) (PVDF) and its copolymers with trifluoro-ethylene [P(VDF-TrFE)] present exceptional material advantages like flexibility, processability,[1] excellent chemical resistance, high mechanical strength, and strong piezoelectric properties[2] to justify their substantial use in various applications. These materials have electromechanical and acoustic applications in sensors, actuators, microphones, hydrophones, and ultrasound transducers.[3] They are also good candidates for data storage devices,[4,5] tactile sensors,[6] solar cells,[7] and energy-harvesting systems.[8]

Now integrated in many micro- and nano-sized electronic devices, the P(VDF-TrFE) films, whose performance optimizations are still under investigation,[9,10] are classically fabricated by chemical solution deposition methods: spin-coating,[11] dip-coating,[12] Langmuir–Blodgett deposition,[13] and, more recently, electrophoretic deposition.[14] Although classically used for smooth and flat thin films, most of these techniques are not suited to the design of complex structures.

This paper focuses on innovative technologies based on inkjet-print fabricated P(VDF-TrFE) films to develop high-frequency (HF) ultrasound transducers. Characterized by higher crystallinity than PVDF and higher piezoelectric response, P(VDF-TrFE) is a particular material candidate for use in HF ultrasound (>20 MHz) because its high bandwidth and sensitivity lead to good quality ultrasound images.[15] A stretching step must be applied to PVDF films to increase its piezoelectric properties (increase the content of the β-phase).[16] For P(VDF-TrFE), this step is often not necessary because it does not significantly increase the final properties.[17] This mechanical step must in any case be applied on a free film such as a membrane, and this is incompatible with our technique where the deposition must be done on a rigid substrate. Moreover, compared to piezoelectric ceramics in ultrasound transducers, P(VDF-TrFE) is more resistant to mechanical shock, more flexible, lighter, low cost, and has the added advantage of good chemical stability and acoustic impedance that is close to that of water and other soft biological tissues.

Published under an exclusive license by AIP Publishing

HF transducers are classically manufactured by bonding a few micrometers thick[18] free P(VDF-TrFE) films on a substrate. However, this intermediate bonding glue layer often leads to a degradation of transducer performance and poor reproducibility in the manufacturing processes. Our study utilizes the P(VDF-TrFE) 3D printing method, proposed by Haque *et al.*,[19] for flexible electronics application to integrated silicon-P(VDF-TrFE) HF transducers. Most importantly, this approach eliminates the bonding step from the P(VDF-TrFE) film manufacturing process and suitable for the fabrication of complex structures. This substrate can be directly used as a backing for HF transducers.

Previously developed with the spin-coating method,[20] the deposition of P(VDF-TrFE) copolymer on silicon substrates allows for the electronics' integration directly in the wafer with complementary metal–oxide–semiconductor (CMOS) technologies. Thus, it would be possible to integrate almost the entire ultrasound system inside an ultrasound probe. In addition to a better footprint, the use of transducers with integrated electronics can overcome defects from electrical cables and increase overall acoustic performance. The latter is particularly true at higher frequencies as transducer performances are often severely degraded by electrical connections, which behaving like inductors, thus form low pass filters with the intrinsic capacity of the active element.

This feasibility study describes, first, the printing process of P(VDF-TrFE) material deposition on silicon, taking into account the technical constraints imposed by the realization of a high-frequency ultrasound transducer. Second, the integration on the printed circuit board (PCB), polarization, and electro-acoustic characterization steps of the device are described. Finally, the acoustic performance of the realized transducer is presented and compared with the literature and theoretical results.

II. FABRICATION PROCESS

The P(VDF-TrFE) printing process described here was developed by Irlynx,[21] using LFoundry's Class 150 nm Analog/Digital CMOS technology (LF15A technology).[22] The applications targeted were low-cost infrared imagers and ultrasonic array transducers. In this implementation, only the last conductive and insulating layers of CMOS process are used for the initial development step.

The substrate used was a CMOS-P silicon wafer [(100) orientation] with a diameter of 200 mm and a thickness of 725 μm. Wafers were first coated with a 2 μm passivation layer of silicon dioxide (SiO_2) to insulate their conductive connections to the substrate and reduce their capacitive coupling. Then, conductive tracks were created by routing and connecting to pads at the bottom electrode of the transducer (Fig. 1). The connections made of a 0.8 μm thick layer of aluminum/copper (AlCu) (0.5% Cu) covered by a thin titanium and titanium nitride Ti/TiN barrier were deposited by sputtering and patterned by photo-stepper and plasma etching. To the step involving the deposition of CMOS LF15A and last passivation layers of silicon monoxide (SiO) and silicon nitride (SiN) was added a specific planarization step to ensure a flat field for subsequent construction steps. Layers of SiO and SiN were deposited by plasma-enhanced chemical vapor deposition (PECVD). The contacts between the Al connection and the bottom electrode of the P(VDF-TrFE) transducer are realized by small arrays of conductive tungsten (W) plug vias (0.4 μm in diameter) through the passivation layers. Vias are photo-etched and then filling by W chemical vapor deposition (CVD). The bottom electrode of the transducer comprised 0.2/0.03 μm thick Ti/TiN. The layer of TiN prevents the natural oxidation of Ti and ensures good electrical contact of the connection between the bottom electrode and pads.

To significantly improve adhesion of the P(VDF-TrFE) to the bottom electrode of the transducer and passivation layers, a 0.1 μm thick layer of polymer resist (CT4000, Fujifilm) with similar properties to polymethyl methacrylate, (PMMA) was deposited by spin coating.[23]

The P(VDF-TrFE) copolymer used in this study comprised 17 mol. % of trifluoro ethylene and 83 mol. % of poly(vinylidene fluoride). This composition allows for optimizing the electromechanical properties, particularly the thickness coupling factor (k_t), a key parameter for transducer applications.[17] Inkjet printing technology used a 2 wt. % solution of P(VDF-TrFE) in dimethyl sulfoxide (DMSO) solvent. The printing solution viscosity measured at 30 Hz was limited to 4 mPa s due to its non-Newtonian behavior during drop ejection through the print-head nozzles.

The P(VDF-TrFE) pattern was produced by the inkjet direct impression method using a digital printer (CeraPrinter F-Serie, CERADROP, MGI). The print head (Sapphire QS-256/30 AAA,

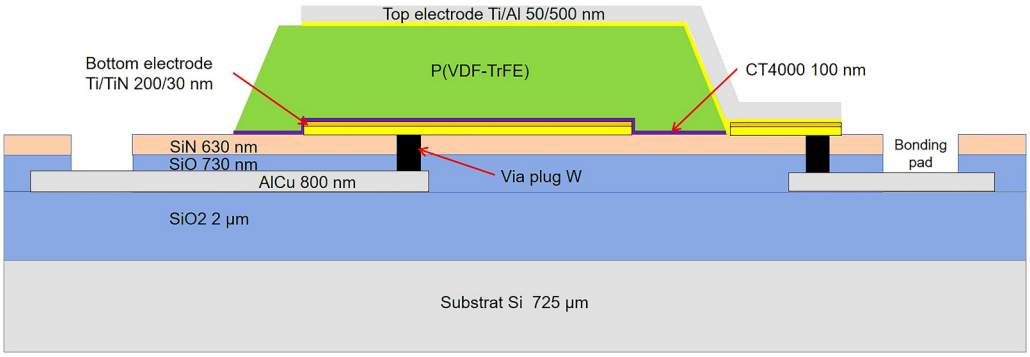

FIG. 1. Cross section of the schematic drawing of the device (not to scale).

Published under an exclusive license by AIP Publishing

Fujifilm) used consisted of 256 aligned nozzles (30 μm in diameter) spaced 254 μm apart. The jetted drops had a typical volume of 50 pl. The process involved a first deposit approximately 50 nm thick, made up of drops spread over a 100–150 μm in diameter. Several deposits were thus superimposed to obtain the desired final thickness. Between 15 and 20 deposits were required per micrometer of dried thickness. The average thickness of each deposit was simply determined by the amount of jetted P(VDF-TrFE) per unit area. Therefore, the average thickness was the same for each deposit independently of the previous deposits, but a certain roughness especially for the very first ones was present. When successively printing P(VDF-TrFE) deposits, the silicon substrate was heated to 70 ± 5 °C, and the print head temperature was 40–45 °C. This temperature regimen allowed for real-time evaporation of the solvent to ensure a homogeneous final layer, devoid of a whole "coffee ring" effect.[24] The printing speed was adjusted so that the solvent could evaporate before the next coating was applied. In order to produce a homogeneous and uniform final layer, these successive depositions were in hexagonal meshes [Fig. 2(a)]. After P(VDF-TrFE) and top electrode deposition, annealing was at 170 °C [temperature above that of P(VDF-TrFE) melting][25] for 30 min. The 170 °C allowed for the crystallization

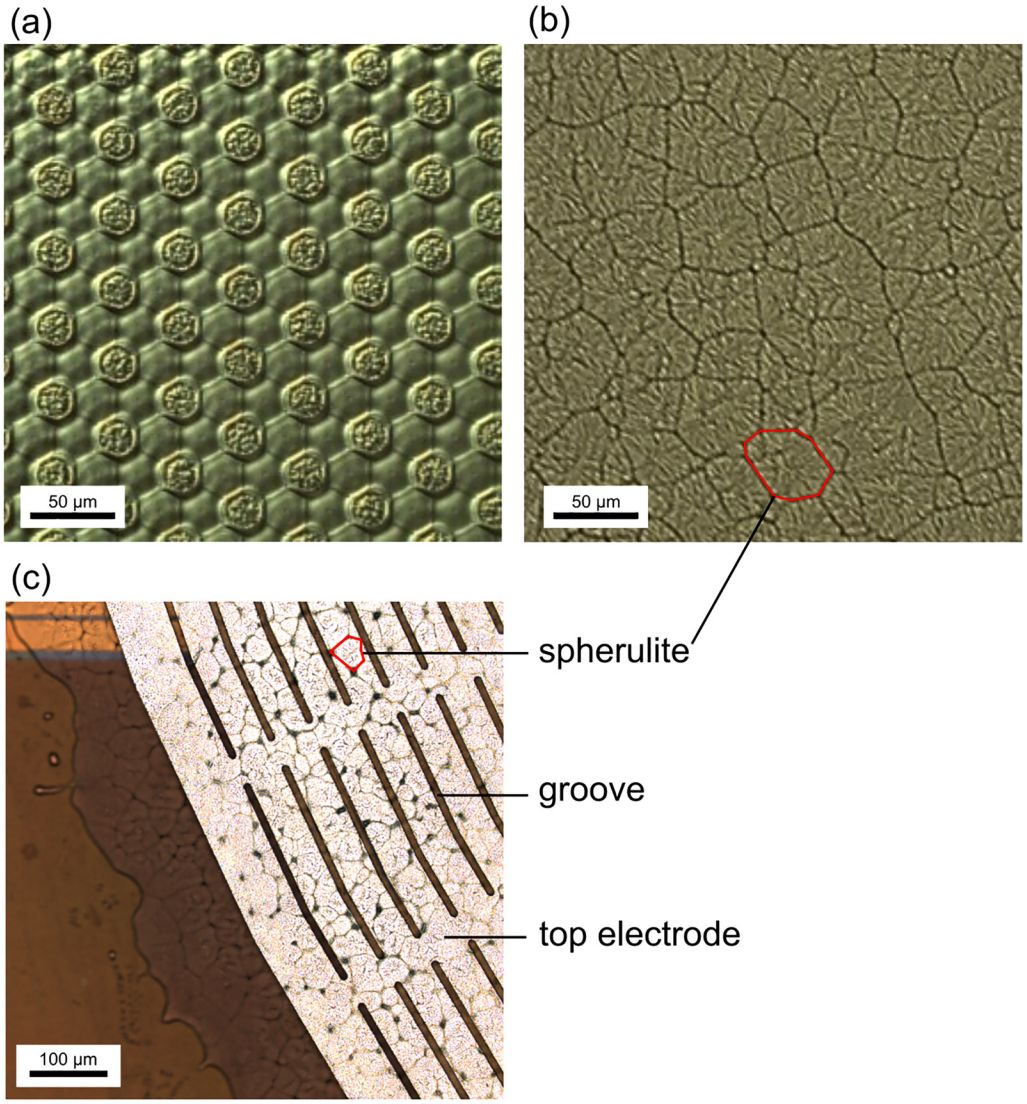

FIG. 2. Optical microscope images of (a) several P(VDF-TrFE) layers with hexagonal meshes for drop deposition before annealing, and (b) after annealing, the drop structure is smoothed; (c) top Ti electrode (edge) with and without the grooves. Below the electrode, the spherulites of P(VDF-TrFE) are observed with a diameter of around 50 μm.

Published under an exclusive license by AIP Publishing

(50%–60%) and residual solvent removal, suppression of drop topology roughness, and any nano- or micro-defaults like pinholes [Fig. 2(b)].

The Ti/Al (0.05/0.5 μm) layer for the top electrode was deposited by sputtering onto the P(VDF-TrFE) film. Here, Ti allows for good adhesion to the copolymer film, while Al reduces its electrical resistance. The top electrode had dimensions of 0.2 mm in width for connections to pads and 2.5 or 7.5 mm diameter for the transducer's common electrode. Structured with groove shaped holes as shown in Fig. 2(c), these electrodes facilitate the degassing of P(VDF-TrFE) without detachment of the electrode and suppress bubbling during annealing. To account for the high step of P(VDF-TrFE) and also obtain a conformal cover (Fig. 1), the 3 μm photo-resist (AZ 4999) was spray-coated using an automated sprayer (Altaspray Süss Microtec). The photo-resist used was made on a proximity EVG 6200 mask-aligner. Etching on metals was wet treated for Al and dry treated for Ti (ICP/RIE Corial 200 mm). Resist stripping used a solvent mixture of ethyl lactate and methyl ethyl ketone (RER500, Fujifilm).

The main advances of this technology involved splitting the processing steps into two phases. In phase one, the processing steps relied on standardized current CMOS fabrication. In phase two, specific materials (like PVDF-TrFE) are produced in a non-constraining design using direct inkjet printing. The process is well adapted for small volume fabrications and all specific steps, easily accomplished by transducer manufacturer.

III. PACKAGING AND POLING

Each full wafer contained 65 identical patterns, cut with a dicing saw. Thickness profiles for a representative chip with a single P(VDF-TrFE) pattern were measured with an optical profilometer (Confocal Microscope OLS40-SU, Olympus). The film showed good thickness uniformity, with a mean thickness of 11.4 μm and a ±5% variation. Before poling and measuring its electrical and acoustic output, the chip was secured on a specifically designed PCB with 25 μm diameter of aluminum wire bonding as electrical connections. A resin (HIPEC® Q1-9239, Dow Corning) of semiconductor protective coating heated to 175 °C for 35 min was applied to the wires to protect their mechanical and dielectric integrities (Fig. 3). A coaxial cable with a characteristic impedance of $Z_c = 50\ \Omega$ was used for the electrical connections to the chip, through specific pads designed on the PCB. Poling involved applying a 135 V/μm electric field between the bottom and top electrodes of the P(VDF-TrFE) film and inducing the piezoelectric activity. The poling step was performed in oil at room temperature. The polarization cycle consisted of three bipolar sinusoids having a frequency of 50 mHz. This procedure is based on the previous studies already described by Bauer *et al.*[26]

IV. CHARACTERIZATION AND DISCUSSION

A. Electromechanical properties of P(VDF-TrFE) film

Electromechanical performances for the copolymer films were deduced from complex electrical impedance measurements, specifically the fundamental thickness-mode resonances. For the

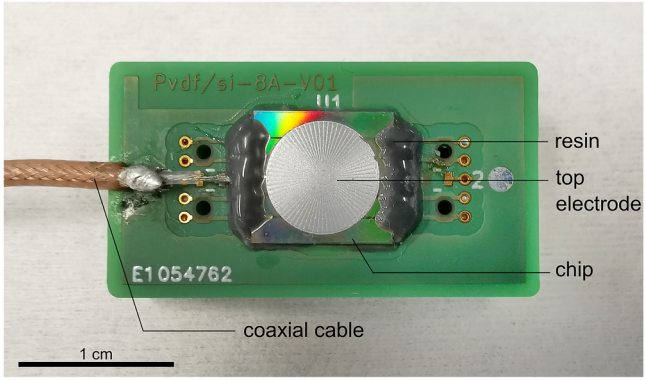

FIG. 3. Photograph of the transducer on a printed circuit board with a top electrode of 7.5 mm diameter.

experimental setup, an impedance analyzer (Agilent 4294A) and an impedance test kit were used to acquire data at the frequency range of 10–85 MHz. A one-dimensional equivalent electrical circuit model of the Krimholtz–Leedom–Matthaei (KLM) model was used to calculate theoretical impedance corresponding to the same frequency range.[27–29] The deduction of thickness-mode parameters for P(VDF-TrFE) films was from experimental data fitting.[30,31] The device was composed of several layers, shown in Fig. 1, with a piezoelectric layer and eight inert layers (silicon substrate, SiO_2, SiO, SiN, CT4000, and Ti/TiN, Al electrodes). As compared to lateral dimensions of the top electrode, thicknesses for all the layers were low and confirmed that only the thickness-mode need consideration. Most inert layers had lower thicknesses compared with P(VDF-TrFE) and negligible effects on the electrical impedance of the whole multilayer structure except electrodes, which had high acoustical impedance compared to P(VDF-TrFE).[18] Accordingly, only four inert layers, the silicon substrate, the two Ti/TiN electrodes, and the upper Al layers, were considered. Moreover, samples' thickness for the silicon substrates was in the same range as the substrate's ratios of longitudinal wave velocity and the fundamental resonance frequency of the P(VDF-TrFE) film, assuming free resonator conditions. Resonance coupling between the silicon substrate and the P(VDF-TrFE) film led ultimately to several peaks[32] as shown in Fig. 4.

Thickness, acoustic impedance, and acoustic attenuation data for the four inert layers were taken from Bardaine *et al.*[31] These parameters are considered a constant for the fitting process, especially acoustic attenuation in silicon which is low and slightly dispersive. Finally, with this approach, five parameters of the P(VDF-TrFE) film were deduced: the longitudinal wave velocity (V_l), the dielectric constant at constant strain ($\varepsilon_{33}^S/\varepsilon_0$), the effective-thickness coupling factor (k_t), and the mechanical (δ_m) and electrical (δ_e) loss factors. A specific study on similar multilayer structure with a silicon substrate was already performed to quantify the accuracy of the deduced parameters according to that of the input parameters (variations of several percent).[31] Results delivered limited variations of k_t in the order of 1%. Figure 4 shows the experimental and theoretical electrical impedances (after the fitting

Published under an exclusive license by AIP Publishing

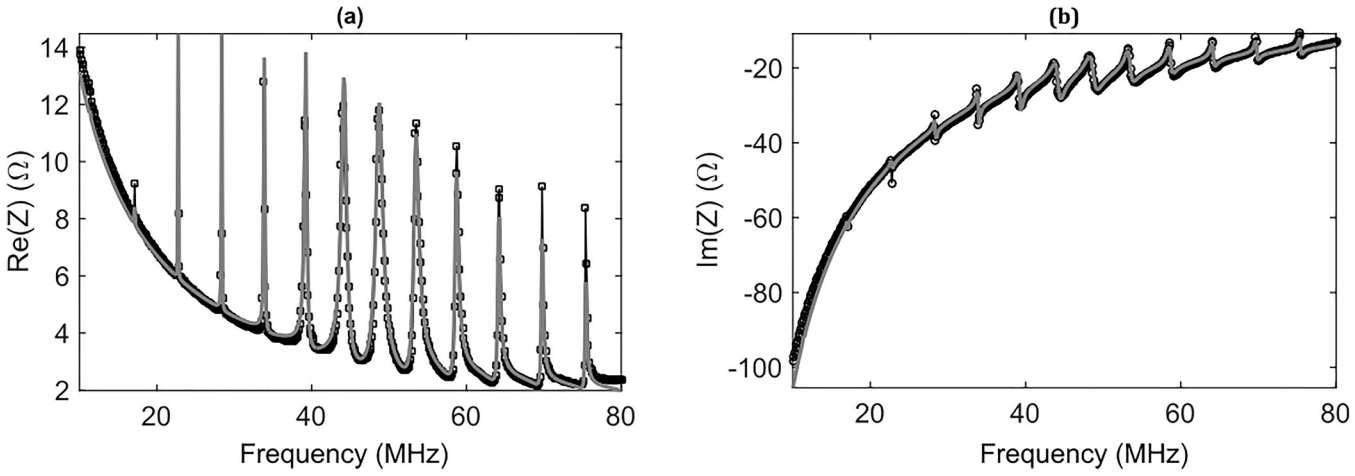

FIG. 4. Real (a) and imaginary (b) parts of the electrical impedance of the multilayer structure with a top electrode of 7.5 mm (black dotted line: experimental, gray solid line: theoretical).

process), while Table I summarizes the deduced parameters. The longitudinal wave velocity (V_l), acoustical impedance (Z), and dielectric constant at constant strain ($\varepsilon^S_{33}/\varepsilon_0$) were comparable to those already obtained in other studies,[17,34] with similar compositions. For the loss factors, the dielectric losses also agreed with literature data[17] measured at 13%, but mechanical losses were higher ($\delta_m = 4.0\%$[34] vs $\delta_m = 3.4\%$[17]) for the inkjet printed material at 9% composition. This higher value can be due to the fabrication process, where a structured material is delivered after inkjet deposition and can be considered an inhomogeneous material, even after annealing. The measured effective-thickness coupling factor for this composition (22%) was lower than that measured for a stretched P(VDF-TrFE) (28.5% for a 72% VDF composition for thicknesses between 20 and 100 μm)[17] but higher than that for PVDF (10%–20%).[18] It should be noted that for these last two films, they were characterized in free mechanical conditions (in air).

B. Ultrasound transducer properties

The characterization of the corresponding transducer was in a water tank filled with degassed water. Pulsing and echo responses were studied using a steel target, positioned 10 mm from the transducer. The transducer was excited with a home-made pulser and receiver incorporating specific emission and broadband reception cards. The pulse excitation generated had amplitudes of 18.3 V spread over 10 ns. This emission voltage will need to be increased for imaging. The amplifier had a speed of 5500 V/μs with a bandwidth of 300 MHz. Tilt angles between the transducer and the steel target were adjusted to maximize the echo amplitude.

Figure 5 shows the electroacoustic responses of the transducer. The transducer had a center frequency (f_c) at 33.2 MHz and a fractional bandwidth (BW) at −6 dB of 100%. With a pulse duration τ_p at −6 dB of 29 ns, the axial resolution (R_{ax}) is 22 μm, calculated from the following equation:

$$R_{ax} = \tau_p \cdot c/2, \tag{1}$$

with c being velocity in water.

The latter value was in good agreement with the approximated expression (2) for axial resolution,[35]

$$R_{ax} = 0.5\lambda/BW = 22\ \mu\text{m}, \tag{2}$$

where λ is the wavelength at the center frequency in water.

Thus, a resonance frequency of this piezoelectric layer that approaches 100 MHz in air (free mechanical conditions) can still

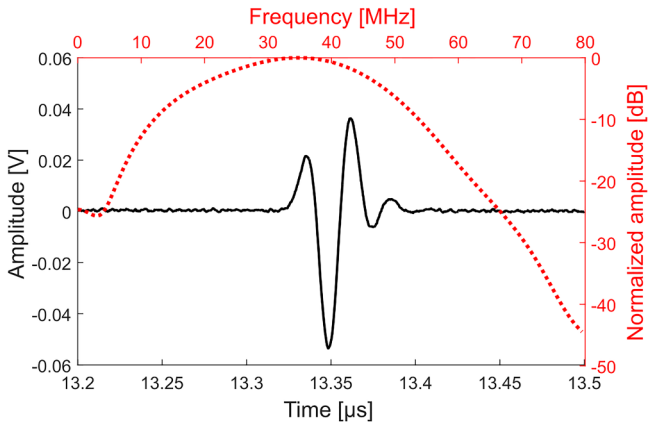

FIG. 5. Time (black solid line) and frequency (red dotted line) electro-acoustic responses measured in water for a transducer with a top electrode of 2.5 mm diameter.

Published under an exclusive license by AIP Publishing

be determined using P(VDF-TrFE) film properties deduced from the KLM scheme. But in the present multilayer structure, the P(VDF-TrFE) film is loaded in the front face with the electrodes and water, which decreases this resonance frequency. Moreover, acoustic impedance of the substrate on the rear face of the film has a strong influence on the resonance wave mode. In our case, the silicon wafer had a much higher acoustical impedance (20.5 MRayl) than the P(VDF-TrFE) film, which led to a ¼ wave resonance.[18] However, considering the many complexities in the fabrication process, this is advantageous since half the number of inkjet printed deposits is necessary for a given resonance frequency. The insertion loss (IL) was deduced from the following relation:

$$\mathrm{IL} = 20 \cdot \log 10(U_e/U_r), \tag{3}$$

where U_e and U_r are the excitation and reception peak voltages, respectively, evaluated from the received voltage in the pulse-echo mode. A gain of 14 dB in reception allowed us to achieve IL = −60 dB. This value is lower than that reported in previous publications,[18,36] although in our case, the bandwidth was higher and the tradeoff between sensitivity/bandwidth was also different.

Radiation patterns were measured in water using a capsule hydrophone (Onda, HGL-0085) with an aperture of 85 μm and calibration to 60 MHz. Connected to a preamplifier with a 20 dB gain, the corresponding signal was viewed on an oscilloscope (Tektronix TDS3034). Measurements involved scanning the axis parallel to the transducer plane at depths ranging from 5 to 60 mm, with iterative 5 mm step changes [Fig. 6(a)]. The diameter of the deposited P(VDF-TrFE) was slightly larger than the diameter of the final electrodes (top and bottom), in order to avoid short circuit between

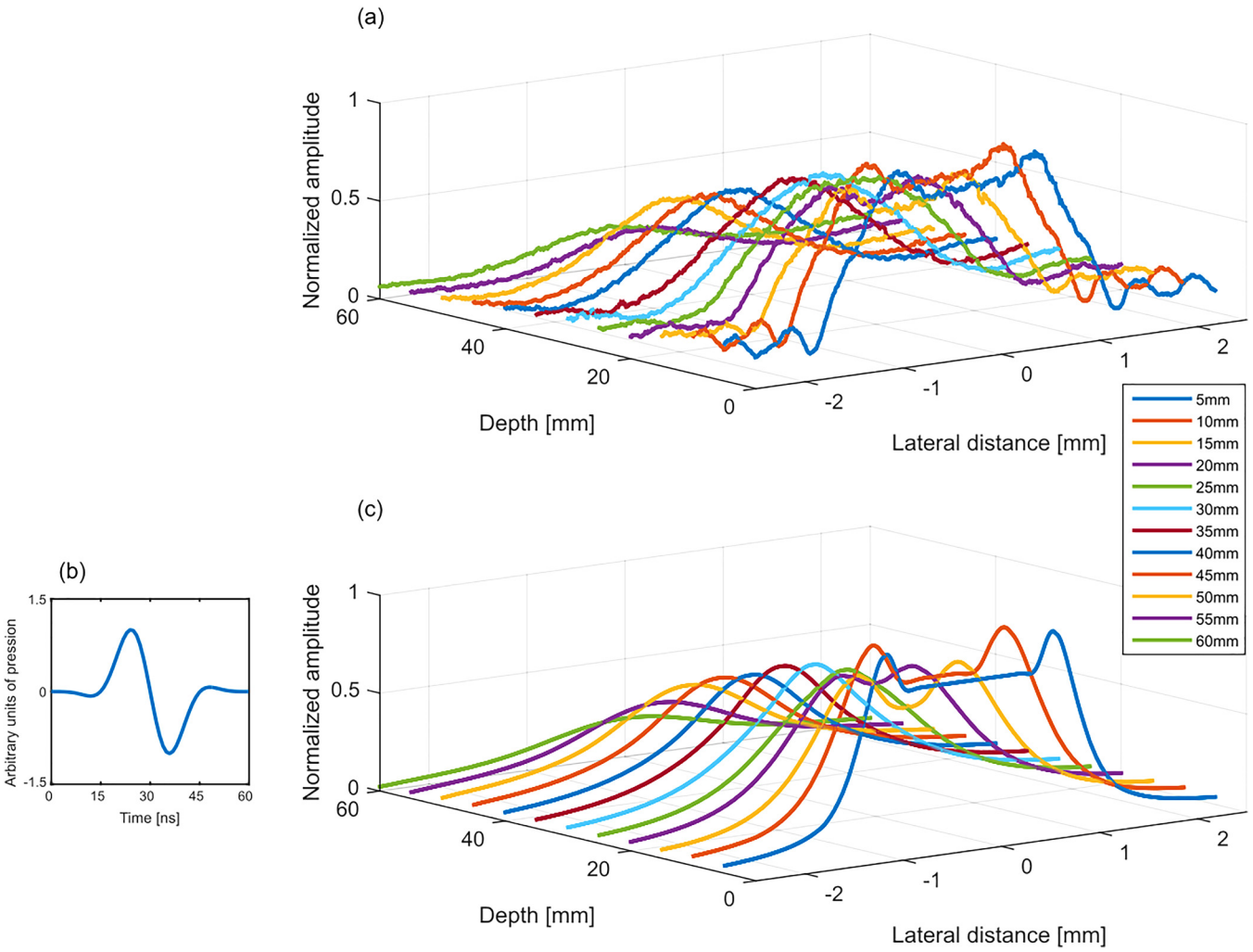

FIG. 6. (a) Experimental of the normalized radiation pattern (pressure) of the transducer (top electrode 2.5 mm) from 5 to 60 mm deep; (b) the theoretical pressure input signal; and (c) the PSTD simulation of the normalized radiation pattern of a transducer (2.5 mm).

Published under an exclusive license by AIP Publishing

the electrodes. During the poling step, a small part of the P(VDF-TrFE) outside the electrode area was also poled and contribute to the sidelobes observed on the experimental results. This effect was enhanced by the presence of electrical contacts.

The numerical axisymmetric model used to determine the transducer radiation pattern in water employed the pseudo-spectral time domain (PSTD) method.[37–39] Spatial derivatives were in the Fourier domain. In our case, wave propagation was in water where no large contrasts of acoustic velocity and density are observable. Consequently, only two nodes per minimum wavelength were required to provide the exact spatial derivatives.[40] Perfectly matched layers (PMLs)[41] were used to avoid reflections on the numerical grid boundaries and counter the wrap-around effect from the FFT. The chosen theoretical pressure input signal had similar characteristics as those for the electro-acoustic response presented in Fig. 5 with a Gaussian shape, a center frequency of 33.2 MHz and a fractional bandwidth at −6 dB of 100% [Fig. 6(b)]. The applied voltage led to a uniform, in-phase deformation of the upper electrode surface with 2.5 mm diameter, corresponding to a one-dimensional vibration mode. The theoretical results in Fig. 6(c) are comparable to pressure measurements. Maximum pressure was measured at a distance of 30 mm from the P(VDF-TrFE) film and shown to be close to the near field limit for a piston mode[42] following the measurement step. These results show that the printed inkjet P(VDF-TrFE) film can act as a homogeneous layer from an acoustic point of view and that the structured top electrode does not have any influence on the radiation pattern.

V. CONCLUSIONS

The 30 MHz high-frequency transducer presented in this paper employed an innovative inkjet-printing of P(VDF-TrFE) films on a silicon substrate as a fabrication process. The optimized step-by-step fabrication process produced a uniform P(VDF-TrFE) film with good electromechanical performance and a thickness coupling factor of 22%. Ultimately, an efficient ultrasonic transducer with low axial resolution (22 μm), high bandwidth (100%), and satisfactory sensitivity was obtained. This technology allowed us to control with high accuracy the thickness of P(VDF-TrFE) film deposition and the center frequency of the corresponding transducer. Moreover, contrary to chemical compatibilities at high temperatures limiting the substrate choice for the ceramic-based thick film fabrication process (type PZT, around 1000 °C), the fabrication process described in this publication does not require high-temperature treatment.

These characteristics allow us to consider medical imaging applications. The sensitivity could be improved by increasing the active diameter of the transducer. Moreover, for these targeted applications, the addition of a lens will be necessary to focus the acoustic beam. Beyond the single-element structures presented here, this technology opens the way for realizing more complex structural arrays, such as multi-element annular or linear arrays, for which element design will ultimately require the patterning of the electrodes (Kerfless structure). P(VDF-TrFE) is a material already recognized for minimizing coupling between elements.[36] Moreover, its deposition on silicon wafers allows for the direct integration of electronics into the substrates, a critical requirement for miniaturization while maintaining good device performance. In this study, a silicon wafer with limited thickness was considered and used as transducer backing. High acoustic attenuation is a prerequisite for the consideration of this element as a semi-infinite medium. For dense silicon wafers, attenuation is low but porosity introduction in the silicon wafer[43] could significantly increase this parameter and allow its use as a backing while also retaining the possibility of electronic integration.

ACKNOWLEDGMENTS

The authors gratefully acknowledge the assistance of Emilie Bahette and Camille Compère (Irlynx) for P(VDF-TrFE) deposition, Flavien Barcella and Laurent Colin (University of Tours) for the electrical connections used on the device, and Jean-Yves Tartu (University of Tours) for the experimental setup of the acoustic measurements. The authors would like to thank the French CERTeM Technological Platform for technological support.

DATA AVAILABILITY

The data that support the findings of this study are available from the corresponding author upon reasonable request.

REFERENCES

[1]D. C. Bassett, *Developments in Crystalline Polymers—1* (Springer, Netherlands, 1982).
[2]H. Kawai, Jpn. J. Appl. Phys. **8**, 975 (1969).
[3]A. J. Lovinger, Science **220**, 1115 (1983).
[4]K. Asadi, M. Li, N. Stingelin, P. W. M. Blom, and D. M. de Leeuw, Appl. Phys. Lett. **97**, 193308 (2010).
[5]R. C. G. Naber, K. Asadi, P. W. M. Blom, D. M. de Leeuw, and B. de Boer, Adv. Mater. **22**, 933 (2010).
[6]C. Li, P. Wu, S. Lee, A. Gorton, M. J. Schulz, and C. H. Ahn, J. Microelectromech. Syst. **17**, 334 (2008).
[7]Y. Y. Choi, K. Kwak, J. W. Seo, M. Park, H. Paik, J. Y. Lee, J. Hong, and K. No, J. Appl. Polym. Sci. **132**, 41230 (2014).
[8]G. W. Taylor, J. R. Burns, S. A. Kammann, W. B. Powers, and T. R. Welsh, IEEE J. Ocean Eng. **26**, 539 (2001).
[9]N. Spampinato, J. Maiz, G. Portale, M. Maglione, G. Hadziioannou, and E. Pavlopoulou, Polymer **149**, 66 (2018).
[10]Q. Sun, W. Xia, Y. Liu, P. Ren, X. Tian, and T. Hu, IEEE Trans. Ultrason. Ferroelectr. Freq. Control **67**, 975 (2020).
[11]Y. Kim, S. Hong, S. Oh, Y.-Y. Choi, H. Choi, and K. No, Electron. Mater. Lett. **11**, 586 (2015).
[12]D. Kim, S. Hong, D. Li, H. S. Roh, G. Ahn, J. Kim, M. Park, J. Hong, T. Sung, and K. No, RSC Adv. **3**, 3194 (2013).
[13]M. Bai and S. Ducharme, Appl. Phys. Lett. **85**, 3528 (2004).
[14]J. Ryu, K. No, Y. Kim, E. Park, and S. Hong, Sci. Rep. **6**, 36176 (2016).
[15]F. S. Foster, K. A. Harasiewicz, and M. D. Sherar, IEEE Trans. Ultrason. Ferroelectr. Freq. Control **47**, 1363 (2000).
[16]L. Li, M. Zhang, M. Rong, and W. Ruan, RSC Adv. **4**, 3938 (2013).
[17]K. Koga and H. Ohigashi, J. Appl. Phys. **59**, 2142 (1986).
[18]M. D. Sherar and F. S. Foster, Ultrason. Imaging **11**, 75 (1989).
[19]R. I. Haque, R. Vié, M. Germainy, L. Valbin, P. Benaben, and X. Boddaert, Flexible Printed Electron. **1**, 015001 (2015).
[20]S.-W. Jung, S.-M. Yoon, S. Y. Kang, and B.-G. Yu, Integr. Ferroelectr. **100**, 198 (2008).
[21]See https://peoplesense.irlynx.com for more information about Irlynx (2020).
[22]See https://www.lfoundry.com for more information about LFoundry (2020).
[23]L. Fritsch, P. Gibert, and C. Vacher, WIPO patent 2009083416A1 (2009).

Published under an exclusive license by AIP Publishing

[24]D. Mampallil and H. B. Eral, Adv. Colloid Interface Sci. **252**, 38 (2018).
[25]C. Vacher, "Intégration Du Copolymères P(VDF-TrFE) à Une Nouvelle Technologie de Capteurs Pyroélectriques: Application à La Détection d'empreintes Digitales," Ph.D. thesis (Université Montpellier, 2007), p. 2.
[26]F. Bauer, Ferroelectrics **49**, 231 (1983).
[27]R. Krimholtz, D. A. Leedom, and G. L. Matthaei, Electron. Lett. **6**, 398 (1970).
[28]S. J. H. Van Kervel and J. M. Thijssen, Ultrasonics **21**, 134 (1983).
[29]M. Lethiecq, F. Patat, L. Pourcelot, and L. P. Tran-Huu-Hue, IEEE Trans. Ultrason. Ferroelectr. Freq. Control **40**, 232 (1993).
[30]P. Marechal, F. Levassort, J. Holc, L. Tran-Huu-Hue, M. Kosec, and M. Lethiecq, IEEE Trans. Ultrason. Ferroelectr. Freq. Control **53**, 1524 (2006).
[31]A. Bardaine, P. Boy, P. Belleville, O. Acher, and F. Levassort, J. Eur. Ceram. Soc. **28**, 1649 (2008).
[32]M. Lukacs, T. Olding, M. Sayer, R. Tasker, and S. Sherrit, J. Appl. Phys. **85**, 2835 (1999).
[33]E. Bellet-Amalric and J. F. Legrand, Eur. Phys. J. B **3**, 225 (1998).
[34]F. Levassort, L. P. Tran Huu Hue, G. Feuillard, and M. Lethiecq, Ultrasonics **36**, 41 (1998).
[35]F. S. Foster, C. J. Pavlin, K. A. Harasiewicz, D. A. Christopher, and D. H. Turnbull, Ultrasound Med. Biol. **26**, 1 (2000).
[36]J. A. Ketterling, F. L. Lizzi, O. Aristizábal, and D. H. Turnbull, IEEE Trans. Ultrason. Ferroelectr. Freq. Control **52**, 672 (2005).
[37]H.-O. Kreiss and J. Oliger, Tellus **24**, 199 (1972).
[38]M. Ghrist, B. Fornberg, and T. A. Driscoll, SIAM J. Numer. Anal. **38**, 718 (2000).
[39]C. Batifol, S. Calle, P. Marechal, M. Lethiecq, and F. Levassort, in *IEEE Ultrasonics Symposium, 2005* (IEEE, 2005), pp. 1660–1663.
[40]Q. H. Liu, Microw. Opt. Technol. Lett. **15**, 158 (1997).
[41]J.-P. Berenger, J. Comput. Phys. **114**, 185 (1994).
[42]E. Dieulesaint and E. Royer, *Ondes élastiques dans les solides. Tome 1, Propagation libre et guidée* (Elsevier Masson, Paris, 1996).
[43]J. Lascaud, T. Defforge, G. Gautier, and D. Certon, Ultrasonics **96**, 196 (2019).

Published under an exclusive license by AIP Publishing